



Jakob Bjerager



Michael Larsen

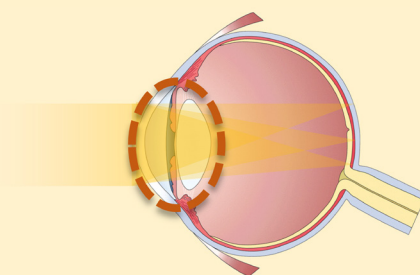
# Refractive riddles and surprises: How far can you get with *ocular aberrometry*?

Jakob Bjerager, MD & Michael Larsen, professor, MD, DMSc,  
Department of Ophthalmology, Rigshospitalet, Denmark

## Refractive riddle

### *noun*

A visual impairment or disturbance of suspected refractive origin that cannot be objectively documented by routine clinical eye examination.



Complaints of blurred vision may defy the attempt of even experienced ophthalmologists to pinpoint the causal anatomical or functional abnormality. Slit-lamp biomicroscopy, ophthalmoscopy, and visual field examination may show no visible irregularities or indirect clues to the location or character of the problem. One may then be tempted to

proceed to search for evidence of occult retinopathy. The term was originally reserved for retinal dysfunction in an ophthalmoscopically normal retina. However, many elusive retinal diseases, such as the white-dot syndromes and some cases of autoimmune retinopathy, can now be identified from structural abnormalities visible on optical coherence tomography

(OCT). If this fails to produce a diagnosis, a work-up for OCT-occult retinal dysfunction and retrobulbar causes of visual loss may be considered, but before ordering electroretinography, magnetic resonance imaging and other costly procedures, it is worth considering whether **occult refractive dysfunction** might be present. The term occult is used here to designate optical

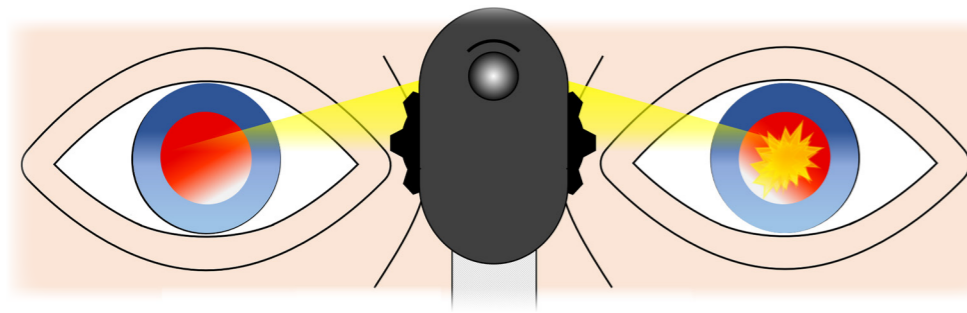


**Figure 1.** Upon slit-lamp biomicroscopy or direct ophthalmoscopy, eyes with clear refractive media and no gross fundus abnormalities will present a clear red reflex (left). In contrast, a cataract will usually disrupt the red reflex (right), but complex aberrations of the lens will not be visible. Thus, a normal fundus reflex does not exclude the possibility that image formation on the retina may be imperfect.

dysfunction that is invisible upon biomicroscopy and direct ophthalmoscopy and that cannot be diagnosed by a standard refractive examination. In some cases, visual acuity testing at

different light intensities may reveal problems related to settings like night-time driving, were double contouring of oncoming headlights are a typical complaint. The addition of a

pinhole to the optimal correction may or may not improve visual acuity, but if the patient sees fluctuations in image quality with small, graded movements of the head, it indicates that refraction

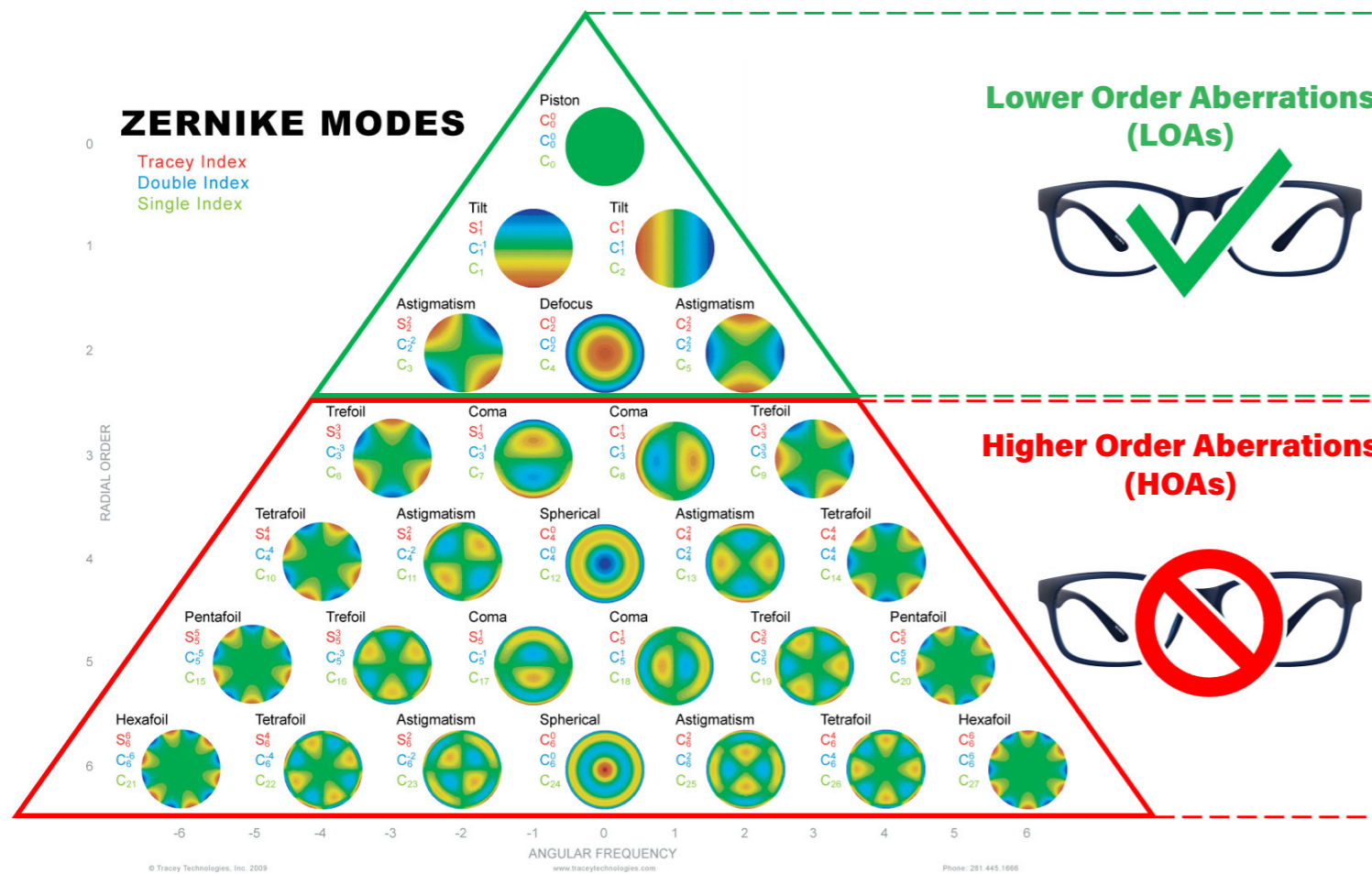


**Figure 2.** Aberration types as classified by Zernike modes. Lower-order aberrations (LOAs) at the top of the pyramidal hierarchy, such as defocus (refractive errors due to sphere) and simple astigmatism (cylindrical refractive errors), can be corrected by prescription glasses. The complexity of higher-order aberrations (HOAs), shown at the base of the pyramid, makes spectacle correction impractical or economically unrealistic. The HOAs of major clinical significance are coma, trefoil, spherical (not to be confused with sphere designating defocus) and secondary (complex) astigmatisms. Illustration adapted from Tracey Technologies Inc., www.traceytech.com.

varies depending on the pupillary aperture.

To settle any remaining uncertainty and to add quantitative evidence, one may turn to **aberrometry**, a tool for refraction mapping that provides advanced measurements and data representation using numbers, graphics, and imaging simulations. It is highly relevant in a situation where one may be considering a surgical intervention in an eye with clear refractive media (**Figure 1**).

**Principles of aberrometry**

Ocular aberrometry adds to subjective refraction with sphere and cylindrical lenses by measuring refraction at multiple locations across the pupil and by summarizing the total refraction over the whole pupil area. A preferred quantitative description begins with spheres and cylinders and then adds **higher-order aberrations (HOAs)** as needed. Aberrations can be quantified by Zernike polynomials, developed by Dutch physicist

Fritz Zernike (1888-1966) who also invented phase-contrast microscopy. Zernike's system is a mathematical description of a hierarchy of geometrically regular optical distortions, of which each type is assigned a root mean square (RMS) wavefront deviation measured in microns ( $\mu$ ). The RMS sum of higher-order aberrations reflects the severity of ocular aberrations that cannot be corrected with defocus and cylindrical components of eyeglasses or contact lenses. Higher-order aberration

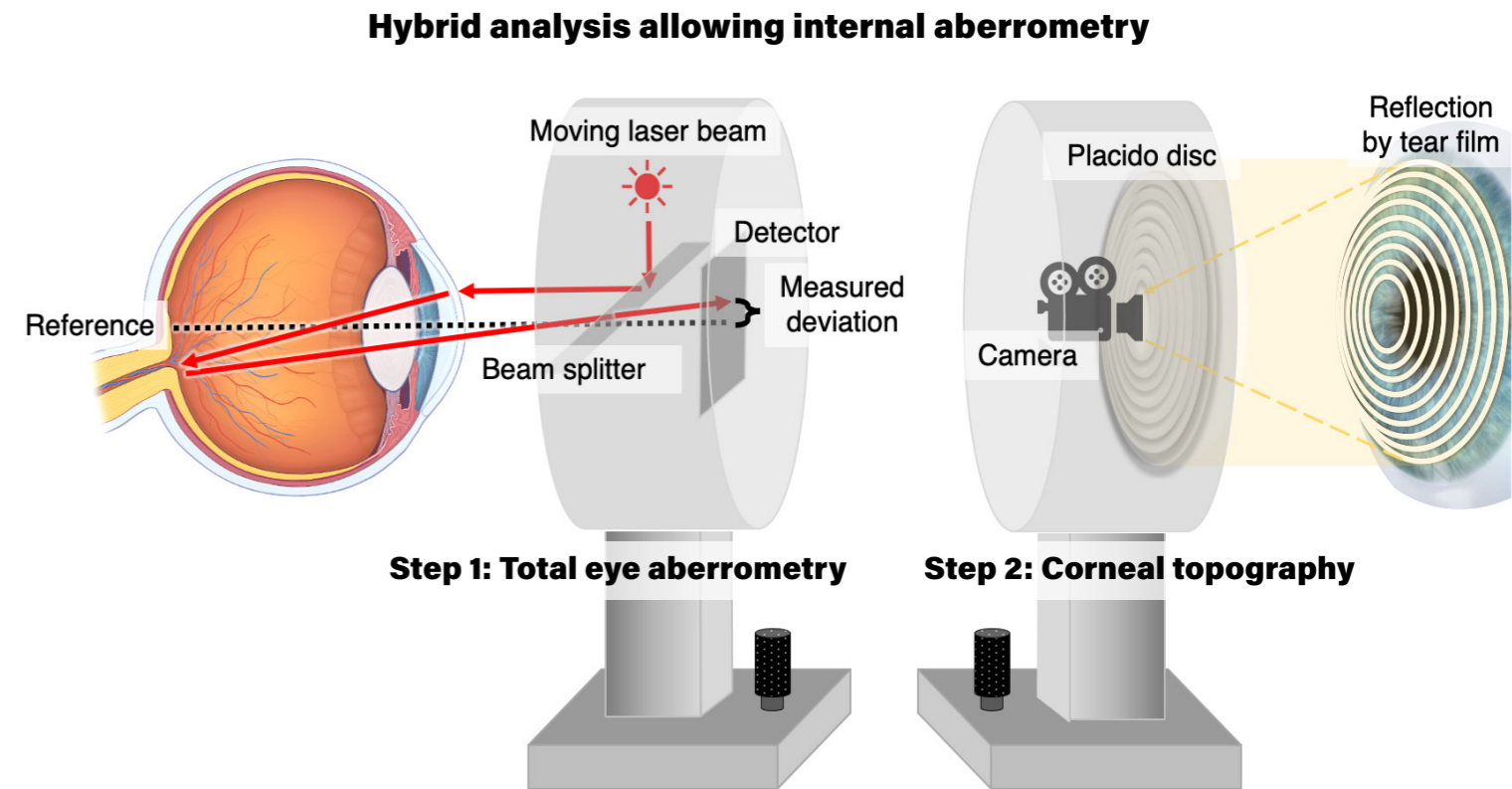


**Figure 3.** The combination of fundus photographic determination of where a given light ray hits the fundus (above left) and information about the orientation of the corneal surface element where the ray entered the eye (above right) allows determination of the contribution to aberrations by separate elements of the refractive system. Subtraction of the surface aberrations found by corneal topography from the aberrations of the whole refractive system calculated by tracing the rays to the fundus yields the sum of internal aberrations. It is then up to the clinician to determine whether the latter are produced by the lens or the posterior cornea. Occasionally, corneal aberrations can be seen to be balanced, wholly or partially, by internal aberrations, which primarily reside in the lens. Preoperative aberration mapping can preempt refractive surprises in such eyes where an imperfect lens is balanced by an inversely imperfect cornea.

RMS sums tend to increase considerably with pupil size, so it is convenient to remember that for a 4 mm pupil diameter an RMS sum above  $0.150 \mu$  is commonly associated with visual complaints.

Zernike modes (Figure 2) are a classification scheme that corresponds well to the majority of optical aberrations found in the human eye. One method of obtaining input data for the fitting of the polynomials is to

use wavefront aberrometry by the Hartmann-Shack principle, in which aberrations are modelled as deformations of an outgoing wavefront. The method is often used in adaptive optics retinal imaging and works well in regular eyes where only moderate aberrations are present. However, there is an inherent risk of wavefront measurement points being confounded at higher levels of aberrations. It is therefore valuable in a clinical

context to have an alternative method that allows for high precision aberrometry in both the common and the more unusual aberrations. One such method is *ray tracing*, which differs from the Hartmann-Shack principle by physically mapping the propagation of multiple parallel ingoing light beams, one beam at a time. We have studied an instrument based on the ray tracing method in research and clinical practice.

**Subject A: Eye with no HOAs**

Ideal retinal spot diagram after optimal sphere correction (-1.6 D)

**Subject B: Eye with high HOAs**

Chaotic retinal spot diagram despite optimal sphere correction (-7.5 D)

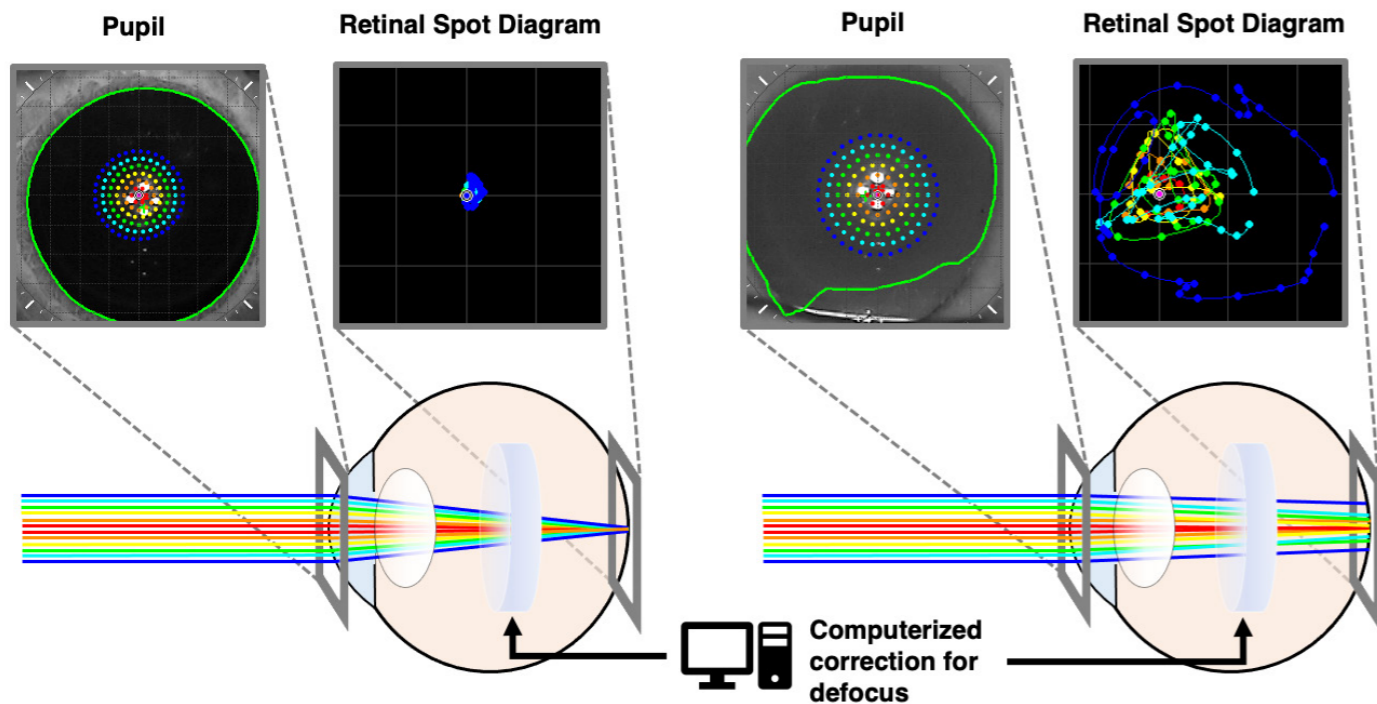


**Figure 4.** The ray tracing aberrometer maps the imaging system of the eye, i.e. its refractive components, over a defined area of the pupil by sending a large number of axis-parallel narrow light beams (rays) into the eye, as indicated by the concentric dotted circles of different colors near the center of the pupils (above). In an unaccommodating and perfectly emmetropic eye, all beams will converge on a single spot or small cluster of spots at the center of the fovea, as seen on the retinal spot diagram of subject A, after automatic correction for myopia of -1.6 diopters (above left). Disorder of the retinal spot diagram that remains after correction for sphere reveals the presence of higher-ordered aberrations in subject B (above right, corrected for defocus -7.5 diopters). Note that spots and beams in the illustration are colored differently solely to discern different measurement eccentricities from the optical axis; in reality a single 785 nm beam is projected consecutively at each of the different axis-parallel positions.

**En face slitlamp image**

A  $0.4 \times 0.7$  mm oval element in the anterior cornea 2 mm inferior to the optical axis.

**Cross-sectional Scheimpflug image**

The same hyperreflective element seen extending 25-175  $\mu$ m below the anterior corneal surface.

**Retinal spot diagram**

Beams that traverse the element deviate to an area inferior of the foveal center

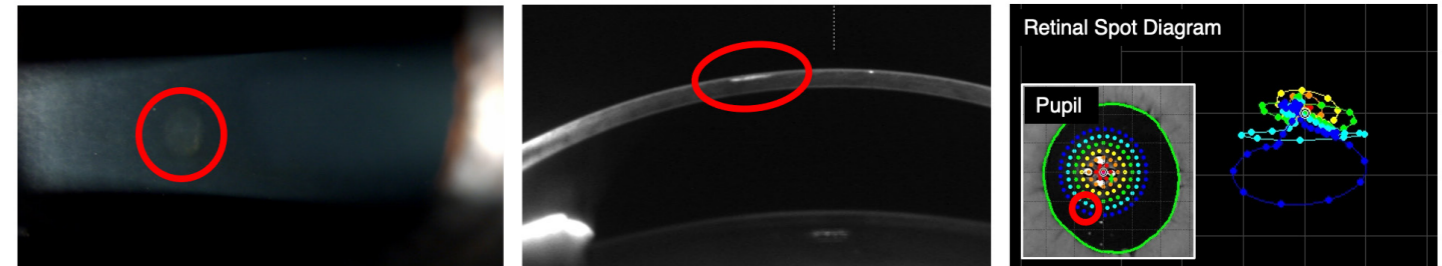


**Figure 5, Case 1.** A 55-year-old man without visual complaints presented for a routine eye examination with best-corrected visual acuity 1.3 Snellen in both eyes. Both lenses were clear. Biomicroscopy showed a semi-transparent opacity, possibly a retained mineral oil droplet, in the anterior corneal stroma slightly inferior to the corneal apex (red markings). He recalled a trauma in his youth where the eye was hit by the greasy tip of a steel wire. The aberrometer found only negligible levels of higher-order aberrations at the surface of the cornea, but there were significant internal higher-order aberrations of  $0.250 \mu$ . The case illustrates how the method of the device inherently divides the analysis of ocular aberrations into those that originate from the very surface of the eye, i.e. the interface between the atmosphere and the tear film, and those that are found anywhere beyond that interface.

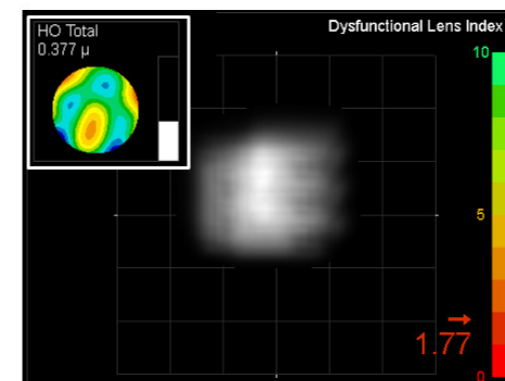
The instrument (iTrace, Tracey Technologies Inc., Houston, Texas, USA) contains a laser beam projector, a fundus camera, and a corneal topographer (Figure 3). The laser beam is rapidly shifted between 256 different axis-parallel positions (Figure 4). The individual path through the eye of each beam

(or ray) is calculated from the information about where it struck the tear film and where it was seen to hit the fundus. This way the refractive properties of the eye are mapped in 250 milliseconds. The local curvature of each corneal surface element, where a given beam has entered the eye, is then measured by

Placido disc topography.

The combined analysis of total eye aberrometry and corneal topography allows for the separation of refraction into anterior corneal and internal ocular indices. Internal refraction is dominated by the lens, or a substitute thereof, and this element is also the most common

**Before cataract surgery**



**After cataract surgery**

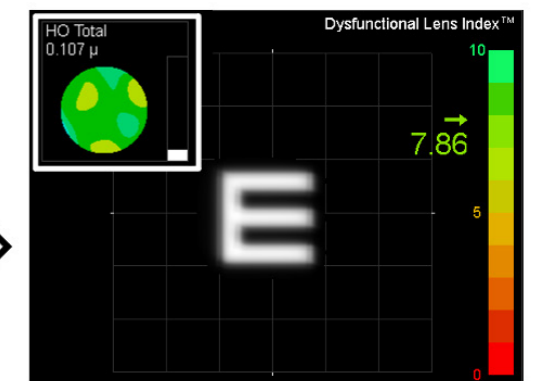


**Figure 6, Case 2.** A 63-year-old man presented with blurred vision, unilateral polyopia, and best-corrected visual acuity 0.25 Snellen in his right eye a few months after suffering a blow-out fracture to his right orbit. Biomicroscopy found no cataract, but internal aberration analysis showed chaotic higher-order aberrations in the eye and severe blurring of the image projected on the retina (above left). Cataract surgery with intraocular lens implantation resulted in a reduction of higher-order aberrations, from  $0.377 \mu$  to  $0.107 \mu$  (inserts, above), resulting in a striking improvement in simulated image quality (above right) and best-corrected visual acuity increased to 1.2 Snellen. The dysfunctional lens index improved from 1.8 to 7.9 on a scale from 0 to 10 after cataract surgery.

source of clinical problems. It is important to understand, however, that aberrations originating from any point behind the surface of the tear film will be labelled 'internal,' as is illustrated by Case 1 (Figure 5).

Intraocular aberrations derived from corneal mapping and ocular ray tracing have shown considerable agreement with subjective vision and cataract severity scores.<sup>2-4</sup> A large prospective study is required to test for potential superiority of aberrometry over conventional methods

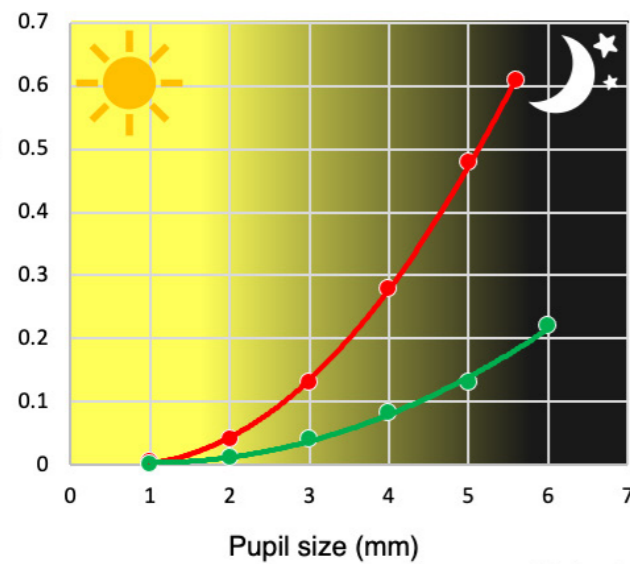
of predicting the outcome of surgery. Meanwhile, clinical utility can be studied on a case-by-case basis.

**Internal aberrations:  
A clinical perspective**

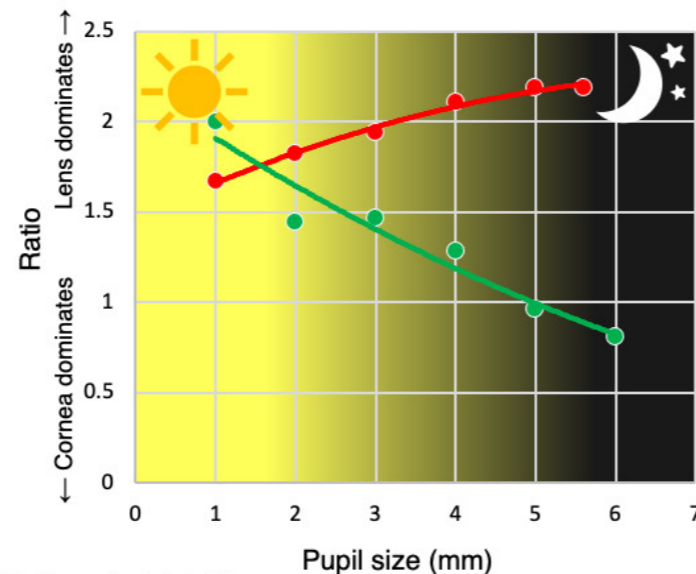
Abnormal refraction in a biomicroscopically clear lens is a classic diagnostic challenge. Internal aberrometry may aid by demonstrating higher-order aberrations induced by dislocation of the lens or by refractile, non-opaque abnormalities in the lens, such as those that occasionally

precede cataract (Figure 6). An added feature of the iTrace aberrometer is a simulation of the image that is projected upon the retina. It can often confirm a patient's complaint of polyopia and be recognized by the patient (Figure 6). This abnormality is summarized in a **dysfunctional lens index** ranging from 0 (worst) to 10 (perfect), which provides a metric of the quality of image formation by the internal refractive components of the eye. A recent clinical study found an association between dysfunctional lens index values

**Internal higher-order aberrations**



**Ratio of internal/corneal surface higher-order aberrations**

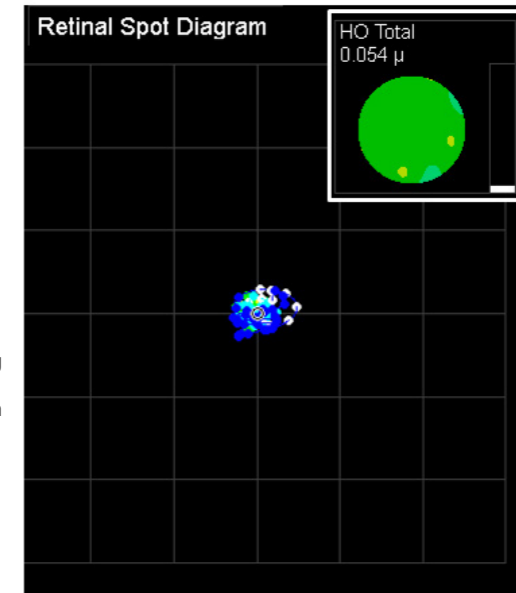


● Patient with blurred night vision  
● Healthy age-matched control

**Figure 7, Case 3.** A 29-year-old phakic woman with myopia -9.5 diopters complained of glare and blurred vision while driving her car at night. In daylight, her best-corrected visual acuity was 1.0 Snellen in both eyes, and she had no visual complaints. Compared to a control subject (green curve), her higher-order aberrations (red curve) increased dramatically with increasing pupil diameter (above left). Contrary to what is normal, her lenses contributed to an increasing fraction of her total higher-order aberrations as pupil diameters increased (above right). Clear lens extraction and implantation of an artificial implant lens, a potential solution for the patient's problem, was not recommended because of the risk of retinal detachment. The patient was satisfied with having been offered an explanation.

**Right eye**

No visual complaints



**Left eye**

CDVA: <0.3

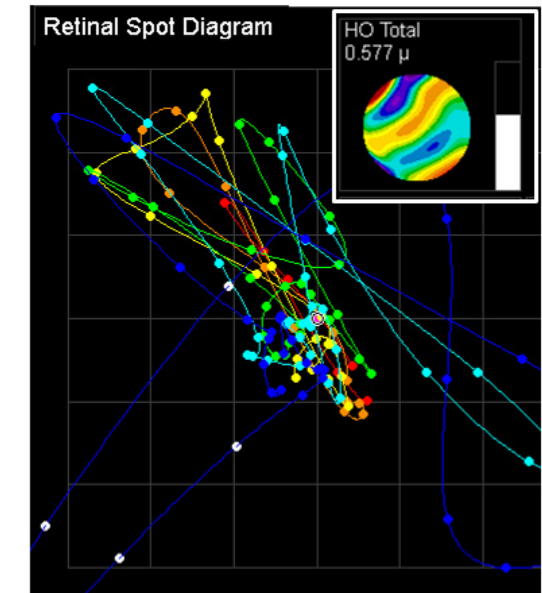
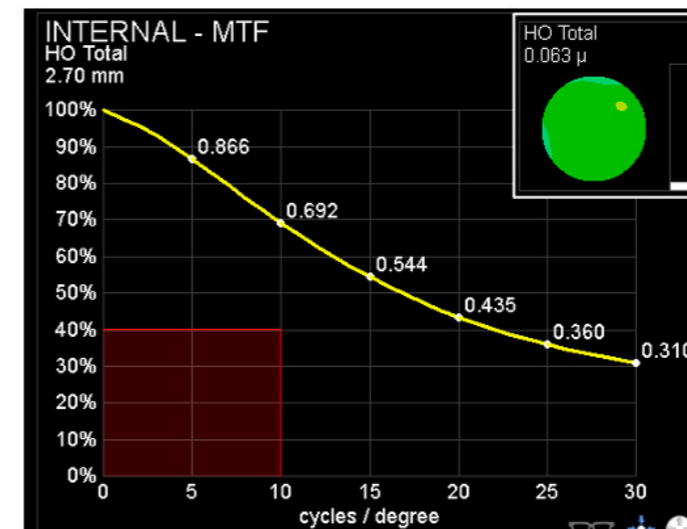


**Figure 8, Case 4.** A 57-year-old man who had undergone cataract surgery with monofocal lens implantation in his left eye 10 years earlier presented with blurred vision of recent onset, monocular triplopia (triple-vision), and best-corrected distance visual acuity <0.3 Snellen in his left eye. His right eye had hardly any higher-order aberrations (insert, left) and the retinal spot diagram was close to ideal (left). In contrast, his left eye had extreme higher-order aberrations of 0.577 μ combined (insert, right), more than 10 times that of the right eye, and a severely distorted retinal spot diagram with an oblique trend (right), supporting the tentative diagnosis of implant lens subluxation. This was difficult to confirm by slit lamp biomicroscopy because his pupils resisted dilation. Surgical intervention confirmed that the implant lens was luxated, presumably due to peripheral capsule rupture. The implant was repositioned and surgically fixed. Visual acuity was normal after surgery.

**Right eye**

CDVA: 1.3



**Left eye**

CDVA: 0.4

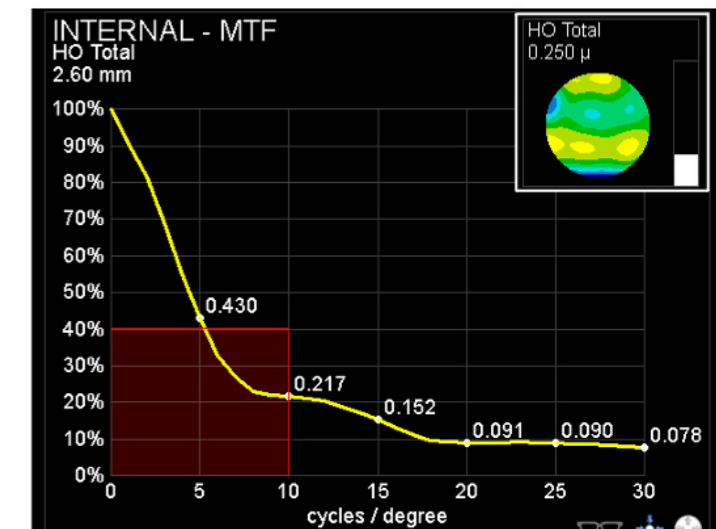


**Figure 9, Case 5.** A 50-year-old man who had undergone successful bilateral cataract surgery with multifocal implant lenses two years earlier presented with blurred vision in his left eye after waking up one morning. Best-corrected distance visual acuity (CDVA) was 1.3 Snellen in his right eye and 0.4 Snellen in his left eye. Biomicroscopy indicated that both implant lenses were well placed in the lens bags. Anterior segment OCT, Scheimpflug imaging, endothelial cell count, fundus photography with OCT, and standard visual field testing were unremarkable. Modulation transfer function curves calculated for the internal refractive components of the patient's eyes showed an acceptable curve for the right eye (left), but an abnormal dip for the left eye at medium and high spatial frequencies (right), down to levels that impair contrast sensitivity (red box). Internal higher-order aberrations in the left eye, at 0.250 μ, were four times higher than in the right eye (above, inserts). Surprisingly, further examination by micropertometric visual field testing showed that the patient had developed a central scotoma and eccentric fixation in his left eye, meaning that his visual axis had shifted away from the original optical axis of the eye. Thus, the axis of the IOL was different from the patient's new, substitute optical axis. The reduction of visual acuity may have comprised both an optical and a sensorineural element.

of 5.6 or lower and a clinical decision to proceed to cataract surgery based on conventional criteria.<sup>2</sup> Due to the nature of ray tracing, the dysfunctional lens index emphasizes disordered refraction rather than diffuse stray light generation, and the

former has been found to be more strongly correlated with subjective vision and objective cataract parameters than the latter.<sup>2-4</sup>

A limitation of visual performance, which is particularly relevant for, but

not limited to, patients who undergo refractive surgery, is that aberrations tend to increase with pupil diameter and thus with low light intensity. The periphery of the eye's refractive system may be of inherently inferior quality, or surgery may have made it out

**The Modulation Transfer Function: A contrast sensitivity measure**

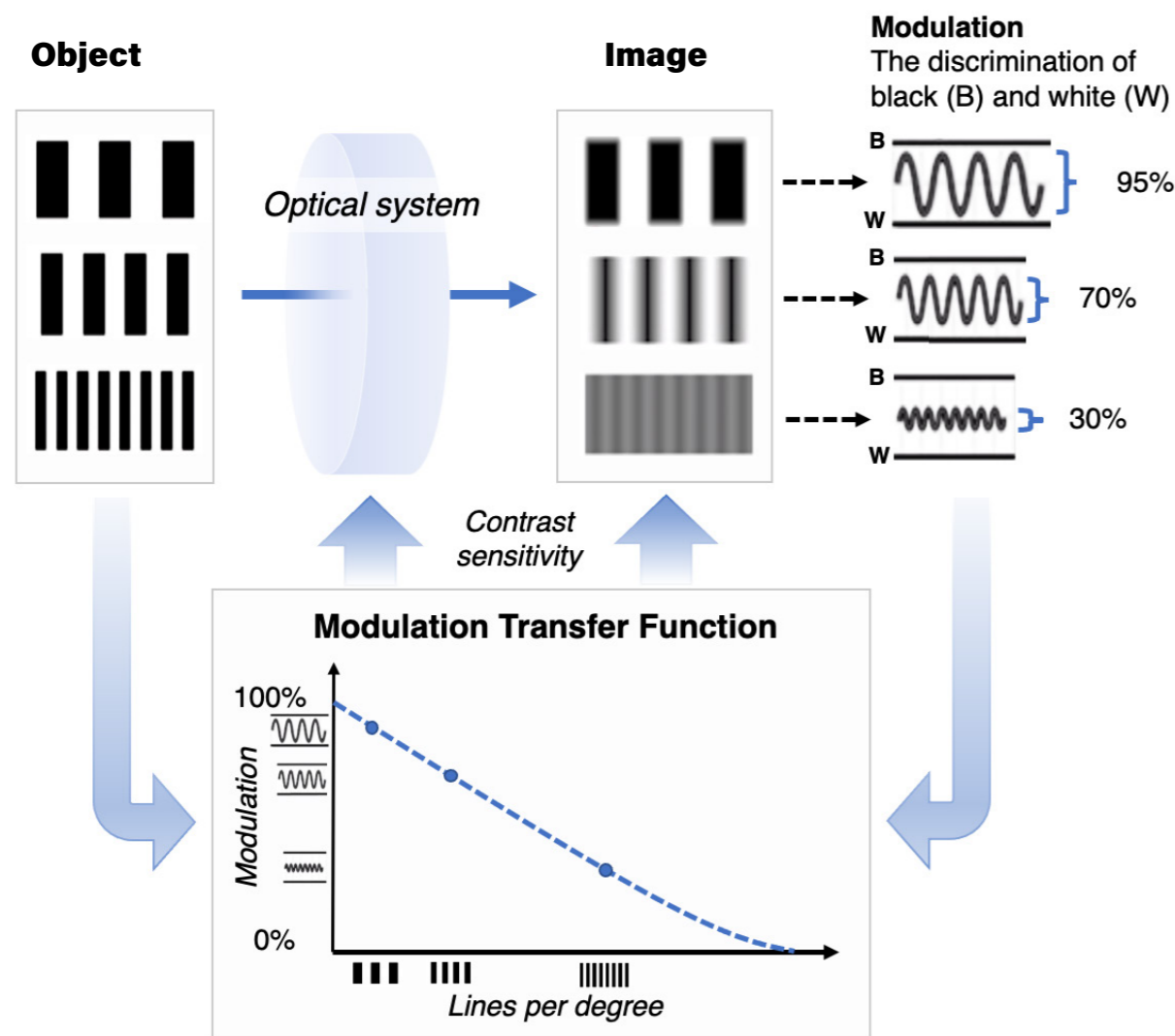


**Figure 10.** Optical imaging systems produce images of limited clarity compared to the original (the object). Imaging quality can be characterized by measuring the degree to which the amplitude and frequency of parallel lines are preserved in an image. The plot of a modulation transfer function (MTF) describes both resolution and contrast and can be defined for the individual components of an imaging system, and the iTrace aberrometer allows the corneal surface element and the rest of the imaging system of the eye to be evaluated separately.

of balance with the central part of the system. This may result in blurred vision and polyopia at night, which can be objectively demonstrated by examining the distribution of a ray tracing retinal spot diagram (Figure 4) or by plotting the sum of higher-order aberrations as a function of pupil size (Figure 7).

Tilt and decentration of intraocular implant lenses can compromise ocular imaging. Objective evaluation can be supplemented by internal aberrometry (Figure 8) and documentation may be valuable, especially if surgical attempts to repair the condition should fail to restore optimal vision.

The performance of a

multifocal type implant lens depends especially heavily upon its proper alignment with the optical axis of the eye. Even slight tilting or decentration can cause blurred vision and markedly reduced contrast sensitivity. Improper axis alignment can be difficult to diagnose by slit lamp biomicroscopy. The aberrometer that we have examined provides a helpful tool in this situation in the form of an algorithm for calculation of the *modulation transfer function* (MTF) for the internal eye (Figure 9). The resulting curve depicts the degree to which contrast of alternating black and white parallel lines is transmitted through an optical system as a

function of the distance between the lines (Figure 10).

Lens anomalies can be found in certain inherited defects of metabolism and connective tissue formation. Prominent types of hereditary lens irregularities include lens luxation, spherophakia, and lenticonus. Their contribution to visual performance can be difficult to evaluate when multiple eye morbidities are present at the same time. In these cases, the mapping of internal higher-order aberrations may help to identify otherwise intangible refractive imperfections and make them amenable to objective empirical study (Figures 11 and 12).

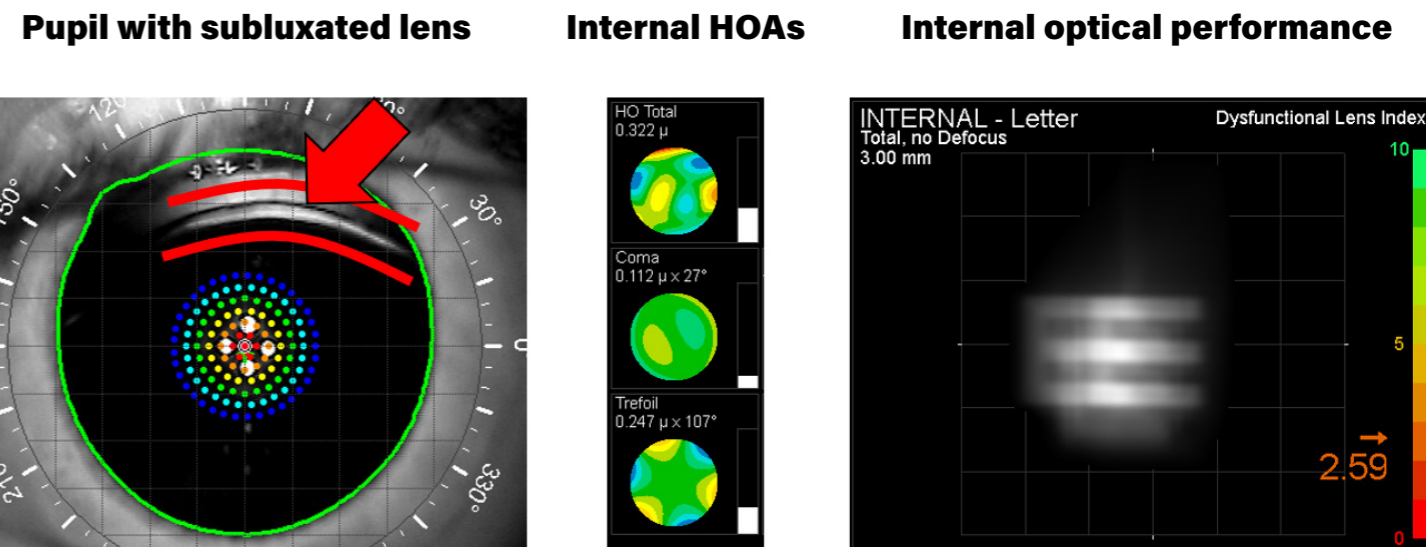


**Figure 11, Case 6.** A 5-year-old child with homocystinuria and spherophakic lenses had a best-corrected visual acuity of 0.3 Snellen in both eyes. Examination revealed a downward subluxation of the patient's right lens, the edge of which was seen in the upper part of the pupil (above left, red arrow). Higher-order aberrations from the lens were of the coma and trefoil types. The higher-order aberration sum of 0.322 μ (above mid), the dysfunctional lens index of 2.59 (above right), and an aberration-free cornea supported the decision to surgically remove the lens, after which aphakic best-corrected visual acuity was 0.6 in both eyes.

**Concluding remarks**

Our preliminary case-based experience with ocular aberrometry, based on the combination of corneal topography and ray tracing analysis, has identified conditions in which this method provides insights or confirms suspicions about reduction in ocular imaging quality. Central to these findings is the ability of the method to separate the relative contributions from the cornea and the lens to optical impairment of vision while simultaneously adding quantitative evidence. A particularly useful application is in the diagnosis of refractive lens dysfunction without opacity. The method will likely also help prevent undue attribution of blurred vision to lens opacities that do not in fact affect vision. Thus, the term lens dysfunction

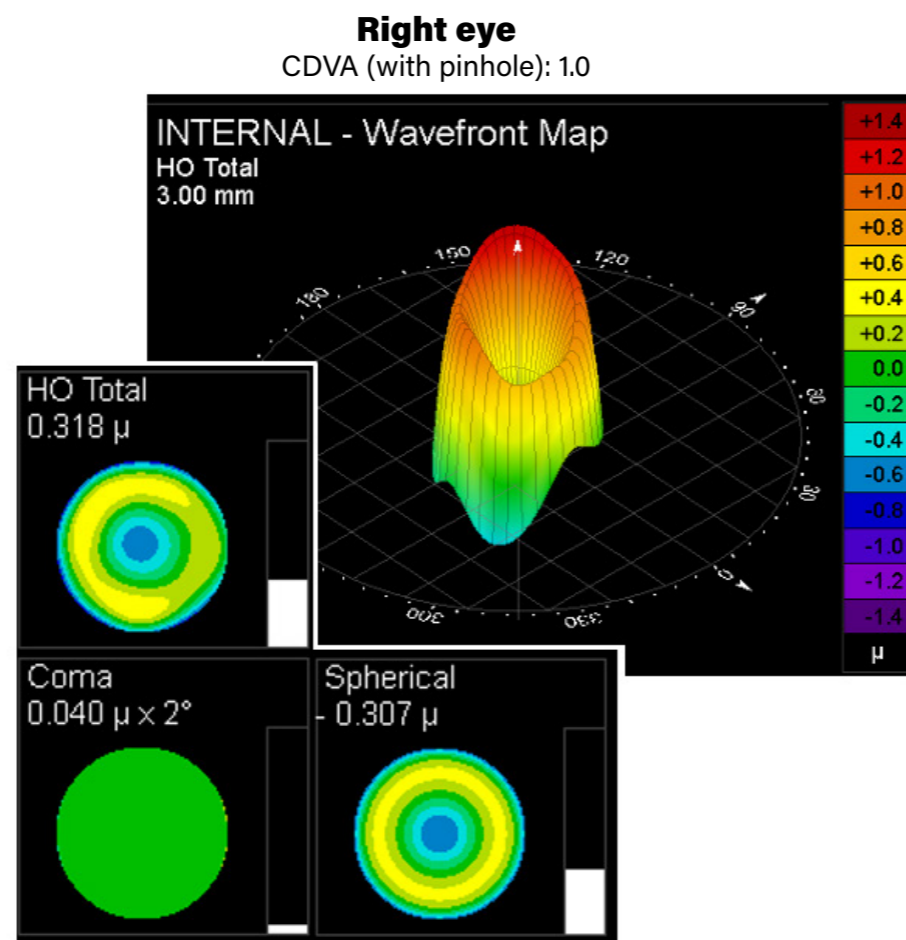
goes beyond cataract to cover clear lenses with internal imperfections of their refractive index gradients or with geometric malformations, as in lenticonus. This is clearly valuable in clinical practice because it helps find explanations and produce documentation when patients are referred with visual loss of unknown origin.

We have found the mapping of internal ocular aberrations to be particularly useful in a multi-subspecialty tertiary eye clinic. The ability to identify or rule out the presence of an

occult refractive problem can accelerate a challenging work-up. We expect that as we gain confidence in the interpretation of data, we may also become more confident in evaluating the relative impact of refractive and sensorineural problems in eyes with co-morbidity.

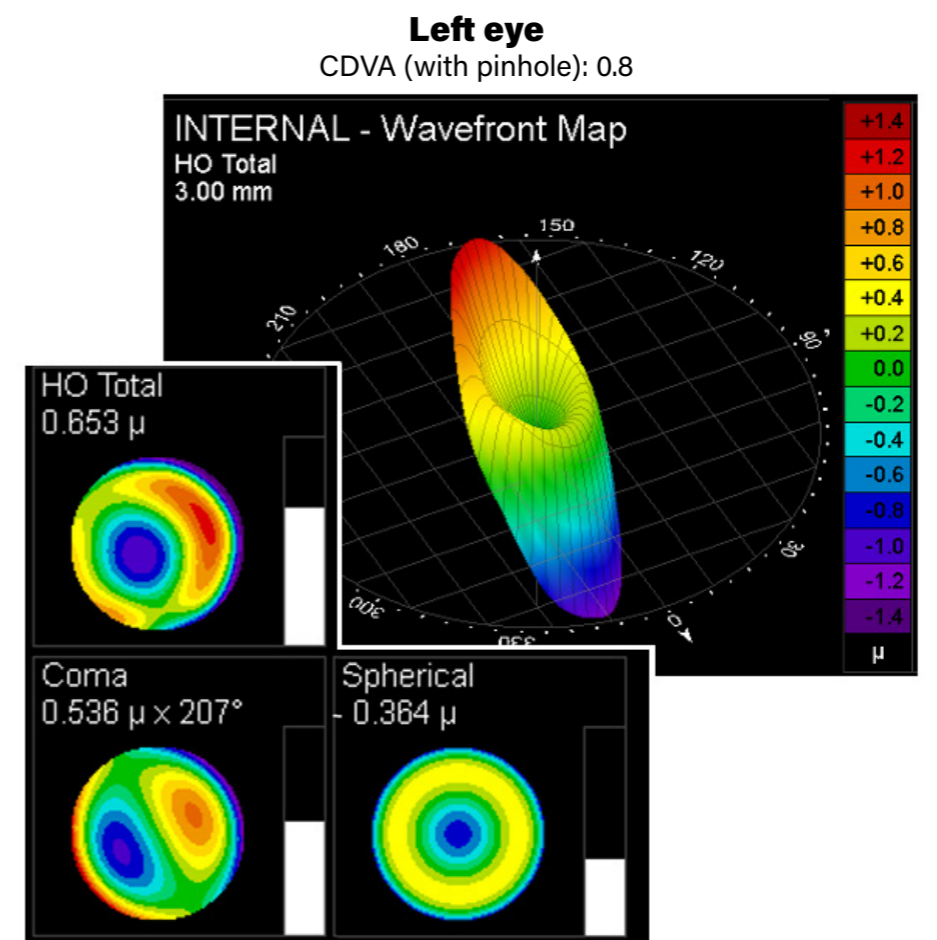
The study of ocular higher-order aberrations is relevant not only for visual performance, but also for fundus imaging, including adaptive optics retinal imaging, which is based on the correction of the higher-order aberrations of the individual eye.

**Figure 12, Case 7.** Internal aberration analysis in Alport syndrome. The patient reported life-long double vision, especially in the left eye, with haze and photophobia. His corneal contours were unremarkable, whereas internal aberrometry showed prominent higher-order aberrations and wavefront distortions compatible with lenticonus. Both eyes had prominent spherical aberration, a higher-order aberration not to be confused with sphere aberration, which is a simple defocus. In addition, there was a coma element in his left eye that added tilt to the volcano-shaped wavefront (right). An ideal wavefront is flat. He habitually squinted to see better and could thereby achieve a binocular best-corrected visual acuity of 1.0. Higher-order aberrations of the spherical type amounted to 0.310  $\mu$  and 0.370  $\mu$  in the right and left eye, respectively, while coma in the left eye amounted to 0.535  $\mu$  (inserts). Coma can be produced by a tilted lens. The left lens was shown by Scheimpflug photography to be intact, but with lenticonus and indeed a significant tilt, possibly due to weakening of the zonules. Alport syndrome is caused by a hereditary collagen defect. Surgery was deferred.



**INTERNAL ABERROMETRY TIPS**

- **Higher-order aberrations increase with increasing distance from the optical axis of the eye.** Measurement diameters are set by the operator and should correspond to pupil diameters that are relevant for the patient, and both eyes both eyes should be measured with the same setting. A measurement diameter of 4 mm is a favored choice for all-round purposes, but larger diameters are valuable for night vision complaints.
- **Not all internal aberrations are produced by the lens.** Everything behind the surface of the tear film counts as internal refraction (Fig. 5, case 1).
- **Pronounced corneal surface abnormalities may compromise reliable measurement of internal aberrations.**
- **Do not jump to conclusions.** Coexisting refractive and sensorineural dysfunction may require a thorough multimodal analysis (Fig. 9, Case 5).



**Acknowledgements:** Nina Jacobsen, MD, PhD, Lotte Falck, MD and Per Riise, MD contributed patient referrals and clinical information. Burton David Kamile, MD, and Kirsten Pearson, MA, provided valuable feedback.

**Conflicts of interest:** The authors have no commercial relations with the suppliers of refractive diagnostic devices or therapeutics.

**Funding:** The study was supported by the European Union under H2020-EU.2.1.1. - INDUSTRIAL LEADERSHIP - Leadership in enabling and industrial technologies - Information and Communication Technologies (ICT) (project ID 780989 MERLIN) ([https://cordis.europa.eu/project/rcn/213189\\_en.html](https://cordis.europa.eu/project/rcn/213189_en.html)). Author J.B. was supported by a pre-graduate research scholarship from THE VELUX FOUNDATIONS (grant no. 00028975, <https://veluxfoundations.dk/en>).

**REFERENCES**

1. Atchison, D. A., Suheimat, M., Mathur, A., Lister, L. J. & Rozema, J. Anterior Corneal, Posterior Corneal, and Lenticular Contributions to Ocular Aberrations. *Invest Ophthalmol Vis Sci* **57**, 5263–5270 (2016).
2. Li, Z. et al. Dysfunctional Lens Index Serves as a Novel Surgery Decision-Maker for Age-Related Nuclear Cataracts. *Curr. Eye Res.* (2019) doi:10.1080/02713683.2019.1584676.
3. Faria-Correia, F. et al. Correlations of Objective Metrics for Quantifying Dysfunctional Lens Syndrome With Visual Acuity and Phacodynamics. *J Refract Surg* **33**, 79–83 (2017).
4. Faria-Correia, F. et al. Comparison of Dysfunctional Lens Index and Scheimpflug Lens Densitometry in the Evaluation of Age-Related Nuclear Cataracts. *J Refract Surg* **32**, 244–248 (2016).